Int Ophthalmol (2019) 39:1061–1069
https://doi.org/10.1007/s10792-018-0909-z

ORIGINAL PAPER

Inter- and intraobserver repeatability and reproducibility of choroidal thickness measurements using two different methods

Angelakis Malamas · Nikolaos Dervenis · Vasileios Kilintzis · Angeliki Chranioti · Fotis Topouzis

Received: 14 November 2017 / Accepted: 22 March 2018 / Published online: 31 March 2018

Abstract

Purpose To measure the inter- and intraobserver repeatability and reproducibility of choroidal thickness measurements taken by the enhanced depth imaging of spectral-domain optical coherence tomography (EDI-OCT) in randomly selected subjects using two different protocols.

Methods Twenty subjects of the Thessaloniki Eye Study database were randomly selected. The participants underwent EDI-OCT, and the choroidal thickness was measured on EDI images using two different protocols. All images were assessed by two examiners independently in two sessions in different days.

Results The interobserver intraclass correlation coefficient (ICC) for average choroidal thickness was 0.944. The average ICC for central, Cmin, and Cmax choroidal thickness was 0.899, 0.863, and 0.955, respectively. The interobserver ICC for average choroidal volume was 0.932. Intraobserver repeatability ICC for grader 1 ranged between 0.925 and 0.9720 and for grader 2 between 0.913 and 0.994.

Conclusion Choroidal thickness measurements by EDI-OCT showed a high inter- and intraobserver reproducibility.

A. Malamas · N. Dervenis · V. Kilintzis · A. Chranioti · F. Topouzis (✉)
Department of Ophthalmology, Aristotle University of Thessaloniki, AHEPA Hospital, St. Kiriakidi 1, 54621 Thessaloniki, Greece
e-mail: ftopouzis@otenet.gr

Keywords Choroidal thickness · EDI · Repeatability

Introduction

The choroid is a highly vascularized structure between the lamina fusca of the sclera and the retinal pigment epithelium. It is composed of the choriocapillaris, the basal membrane of which forms the outer part of Bruch's membrane; the middle layer of medium-sized vessels (Sattler's layer) and the outer layer of large vessels (Haller's layer); and melanocytes interjected between the vessels of Sattler's layer and Haller's layer [1], fibroblasts, resident immunocompetent cells, and supporting collagenous and elastic connective tissue [2]. The choroid plays an important role in providing nutrition and oxygen to the outer layers of the retina. It is a primal site of involvement in various chorioretinal diseases such as central serous chorioretinopathy (CSCR) [3, 4], polypoidal choroidal vasculopathy (PCV) [5–8], age-related macular degeneration (AMD) [5, 6, 8–10], Vogt–Koyanagi–Harada (VKH) [11–13], high myopia [14], white dot syndromes [15], and other chorioretinal disorders. The evaluation of the choroid would be helpful to understand the pathophysiology, diagnosis, and management of these chorioretinal disorders. Thickness measurements have been taken by various studies, but only in selected, commonly subfoveal, points of the macula. Measurements taken at various multiple

single points could be misleading in the overall evaluation of choroidal involvement. Volumetric analysis of the choroid in chorioretinal diseases could be helpful in evaluating the disease course and response to treatment.

Previous studies using various SD-OCT instruments have shown high reproducibility of manual choroidal thickness measurements [16–21]. These studies focus either on healthy subjects [19, 21–24], or on a specific retinal disorder, such as RAP [5, 8, 10], AMD [5, 8, 10, 25, 26], uveitis [27], and diabetes [16, 17, 28]. There is limited evidence regarding choroidal thickness measurements in randomly selected subjects with or without choroidal pathology [20].

Recently, automated choroidal segmentation has been introduced [29–37]. Although automated segmentation represents a step forward, the results of these new attempts fail to clearly establish superiority over manual segmentation. Researchers vary in terms of mean wavelengths used in SD-OCT acquisition. Further, some scans are obtained from young healthy subjects, some from diseased subjects [29, 31, 32], some from adult, and some from pediatric subjects [34]. Moreover, some scans are taken only near the foveal cross section [30, 31], rather than at various locations over a wide range. In addition, a variety of evaluation criteria, including correlation coefficient (CC) [29], Dice coefficient (DC) [30, 31, 34], mean border position difference (MBPD) [29, 33], and mean absolute difference (MAD) [34], have been used. Also, the image quality and subjective complexity appear to differ among various datasets.

This study describes two techniques of manual choroidal segmentation using EDI-OCT Spectralis OCT to obtain choroidal volume and thickness measurements and aims to assess reproducibility and repeatability of these techniques. Our study includes randomly selected subjects from the remaining cohort of the Thessaloniki Eye Study [38], regardless of the presence of choroidal pathology. Thus, our study aims at determining the reproducibility of the above techniques in a population-based setting which would eventually allow the use of these specific techniques in such a research environment involving randomly selected subjects from the general population.

Materials and methods

For this prospective study, 20 eyes of 20 patients (10 males and 10 females) were randomly selected and included from the Thessaloniki Eye Study database. Written informed consent for diagnostic procedures was obtained from each subject before examination. All OCT scans were performed by a single experienced specialist (AM), following pupil dilation with tropicamide 0.5% and phenylephrine 5%. The measurements were taken using the Heidelberg Eye Explorer software (version 6.0.12.0; Heidelberg Engineering Co, Heidelberg, Germany). Spectralis OCT produces up to 40,000 A-scans/sec with a depth resolution of 7 lm in tissue and a transversal resolution of 14 lm by using a superluminescence diode with an 870-nm bandwidth. Two experienced observers (AM and ND) analyzed all scans independently and in two sessions in different days to assess inter- and intraobserver reproducibility.

Choroidal volume imaging protocol

The below image acquisition process and quality criteria were used in all Thessaloniki Eye Study participants. Subjects underwent a single-scan session consisting of a 19-line horizontal raster scan (9 mm length) with 1024 A-scans, 240 μm apart, covering a 30° × 15° area, centered on the fovea. All macular B-scans were acquired in a continuous, automated sequence and were obtained with the automated real-time feature enabled and set to 25 frames. The automated Spectralis segmentation algorithm determines the inner retinal boundary at the inner limiting membrane (ILM) and the outer retinal boundary at the location of Bruch's membrane (BM).

Inclusion criteria were as follows: a) raster image quality > 15, b) raster cube centered on the fovea, and c) in cases where automated retinal boundary error was detected (misplacement of ILM line or misplacement of BM line), manual retinal boundary correction was performed. Significant automated boundary detection error is defined as the misplacement of either of these boundaries continually over a section of scanned retina of 1 mm or greater. Scans were evaluated manually for inner or outer retinal boundary error detection by one experienced observer. When there was a retinal boundary error or a retinal image

misplacement in max 2 raster lines which could not be manually corrected and the defected raster lines were located in different segments of the ETDRS volume measurement map, these raster lines were disabled and the OCT was included [39]. Exclusion criteria were as follows: (a) image quality < 15, (b) raster cube centered off the fovea, and (c) three or more raster lines with retinal boundary detection error. Among those fulfilling the above-described criteria 20 subjects were randomly selected from the Thessaloniki database to be included to this study.

Choroidal image analysis

Two different measurement protocols were used for choroidal segmentation.

According to the first protocol, manual choroidal segmentation was performed following automated retinal layer segmentation software disablement. Masked observers displaced the built-in automated segmentation reference lines from the retinal margins to the choroidal margins. The ILM line was placed onto the outer part of the hyper-reflective line, representing the base of the retinal pigment epithelium. The basement membrane line, which is the reference line for the posterior rim of the retina, was placed onto the posterior rim of the choroid as delimited by the hyper-reflective margin line representing the chorioscleral interface (Fig. 1). This method allowed us to utilize the automatic retinal thickness map features of the built-in software. The automated software allowed choroidal thickness calculations to be made in a similar manner to that for retinal thickness analysis. The standardized grid [40] was placed automatically by the Spectralis OCT software and was visualized through a software designed to map macular thickness (Fig. 1). The standardized grid divided the macula into three circles diameters of 1 mm (central), 3 mm (inner), and 6 mm (outer). We included only the central circle measurements in our study. Values for central average choroidal thickness, central, central min, central max, and choroidal volume were noted (Fig. 2).

According to the second protocol, the horizontal section running through the center of the fovea was selected for analysis. Subfoveal choroidal thickness (SFCT) was defined as the vertical distance from the hyper-reflective line of the BM to the hyper-reflective line of the inner surface of the sclera (Fig. 3). The measurements were taken using the Heidelberg Eye Explorer software [22].

Statistical analysis

Two retina specialists ND (Observer 1) and AM (Observer 2) performed manual choroidal segmentation on choroidal raster scans of each eye on two different sessions. They were masked as to their previous measurements and to each other's measurements. Interobserver agreement was estimated from

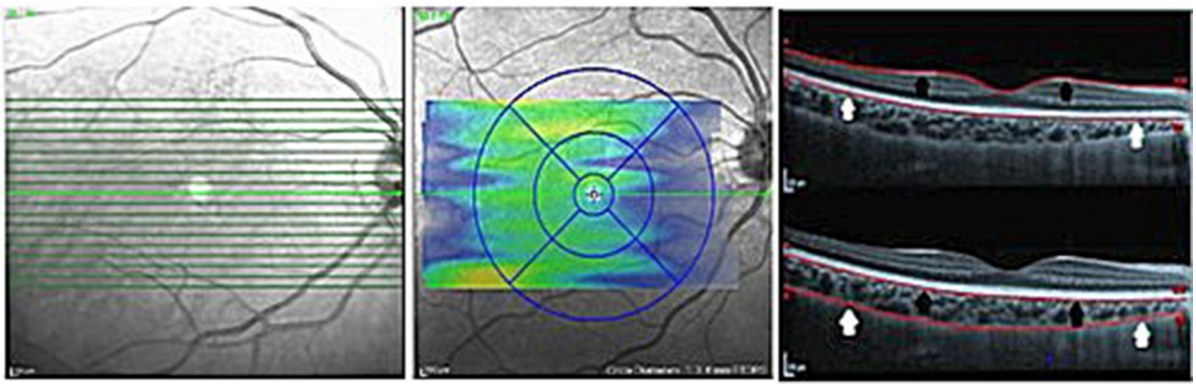

Fig. 1 First measurement protocol. EDI SD-OCT raster scan protocol (left), standardized grid (middle) including three concentric rings with a total of nine subfields centered on the fovea, automated retinal segmentation (right top), and manual choroidal segmentation (right bottom). The internal limiting membrane line (black arrows) and the basement membrane line (white arrows) on automated retinal segmentation were displaced to the base of the retinal pigment epithelium (black arrows) and the chorioscleral interface (white arrows) to demarcate choroidal boundaries (right bottom)

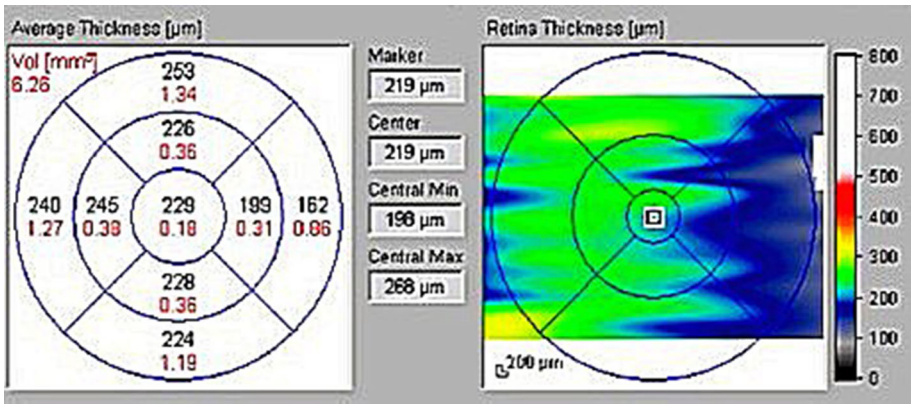

Fig. 2 First measurement protocol. Values for central average choroidal thickness, central, central min, central max, and choroidal volume

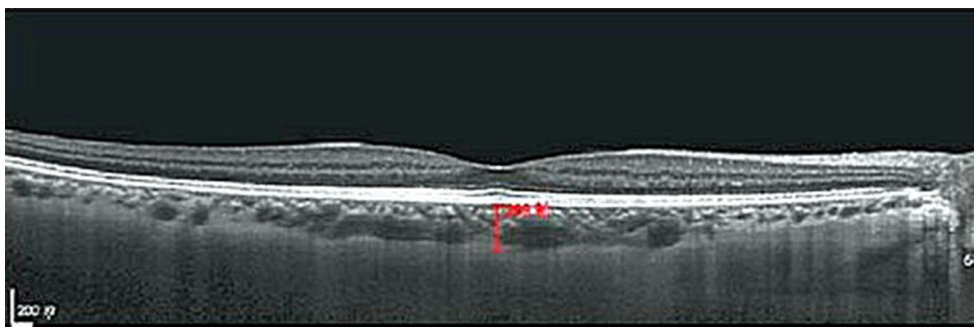

Fig. 3 EDI SD-OCT second measurement protocol. Line of measurement of subfoveal choroidal thickness

the first scan session. Inter- and intraobserver agreement was evaluated for overall average choroidal thickness, average central, central min, central max, total choroidal volume (first protocol measurements), and subfoveal choroidal thickness (second protocol measurements). Agreement between intraobserver and interobserver measurements was assessed using the intraclass correlation coefficient (ICC). Bland–Altman plots were used to evaluate the clinically relevant magnitude of the differences between the measurements and two observers [41]. All statistical analyses were performed with a commercial analytical package (SPSS statistics 21 for Windows; SPSS Inc., IBM, Somers, NY).

Results

This prospective study included 20 eyes of 20 subjects. Mean age was 79.9 years (range 74–85 years), 10 men and 10 women. All subjects were Caucasians (Table 1).

Looking at the first protocol figures, mean average choroidal thickness was 199.50 µm (Observer 1) and 192.45 µm (Observer 2). Mean central choroidal thickness was 199.70 and 199.60 µm, and C_{min} and C_{max} were 166.80, 159.40 µm, and 229.75, 226.35 µm, respectively. Mean choroidal volume was 0.1570 mm^3 (grader 1) and 0.1515 mm^3 (grader 2). The interobserver ICC for average choroidal thickness was 0.944 (95% confidence interval [CI] 0.859–0.978). The average ICC for central, C_{min}, and C_{max} choroidal thickness were 0.899, 0.863, and 0.955, respectively (95%CI 0.745–0.960 for central thickness, 0.655–0.946 for C_{min}, and 0.885–0.982 for C_{max}). The interobserver ICC for average choroidal volume was 0.932 (95% CI between 0.829 and 0.973).

According to the second protocol, mean subfoveal choroidal thickness was 190.85 µm (grader 1) and 190.55 µm (grader 2). ICC figure for average choroidal thickness was 0.960 (95%CI 0.900–0.984)

Table 1 Characteristics of included subjects

	Age	Eye	Sex	SPH	CYL	Axis	Lens
Mean	79.9	10 OD, 10 OS	10 Males and 10 females	0.6	− 0.91	98.6	5 IOL, 15 phakic
SD	3.4			1.9	0.78	37.4	

(Table 2). Bland–Altman plots of mean differences between the two observers' measurements are shown in Fig. 4.

Intraobserver repeatability ICC for grader 1 (ND) ranged between 0.925 and 0.972 and for grader 2 (AM) between 0.913 and 0.994 (Table 3). The results for average, central, C_{min}, C_{max}, volume and second protocol ICC are depicted in detail in Table 3.

Discussion

Before the arrival of enhanced depth OCT imaging, in vivo quantitative assessment of the choroid was not feasible. Ultrasonography was used to assess choroidal thickness prior to ICG angiography, despite low reproducibility. ICG angiography contributed essentially to the understanding of chorioretinal disease [42], but in vivo reproducible estimation of the choroid was still lacking. Reports have been published regarding the reproducibility of choroidal thickness with the use of both the enhanced depth SD-OCT and long-wavelength OCT devices, as well as other commercial spectral-domain non-EDI-OCT instruments [11, 13, 18, 20, 43–46]. These studies reported choroidal thickness at a small number of points, at a single point on vertical and horizontal scans, or used a similar to ours measurement protocol. Quantitative estimation of overall choroidal anatomy, including choroidal volume at the posterior pole and topographic maps of the vascular bed, may provide better insight into macular diseases.

Table 2 Interobserver measurements

$N = 20$	Mean	SD	Values		Intraclass correlation	95% confidence interval	
						Lower bound	Upper bound
N_D_1_avg	199,50	46,003	Avg (μm)	Single measures	894	753	957
A_M_1_avg	192,45	57,099		Average measures	944	859	978
N_D_1_Cen	199,70	46,478	Central (μm)	Single measures	817	594	923
A_M_1_Cen	199,60	63,178		Average measures	899	745	960
N_D_1_C_{min}	166,80	40,674	C_{min} (μm)	Single measures	760	487	897
A_M_1_C_{min}	159,40	46,357		Average measures	863	655	946
N_D_1_C_max	229,75	51,836	C_{max} (μm)	Single measures	913	794	965
A_M_1_C_{max}	226,35	68,903		Average measures	955	885	982
N_D_1_vol	1570	03,629	Vol (mm^3)	Single measures	873	708	948
A_M_1_vol	1515	04,522		Average measures	932	829	973
N_D_2	190,85	44,027	Second protocol (μm)	Single measures	923	817	969
A_M_2	190,55	49,278		Average measures	960	900	984

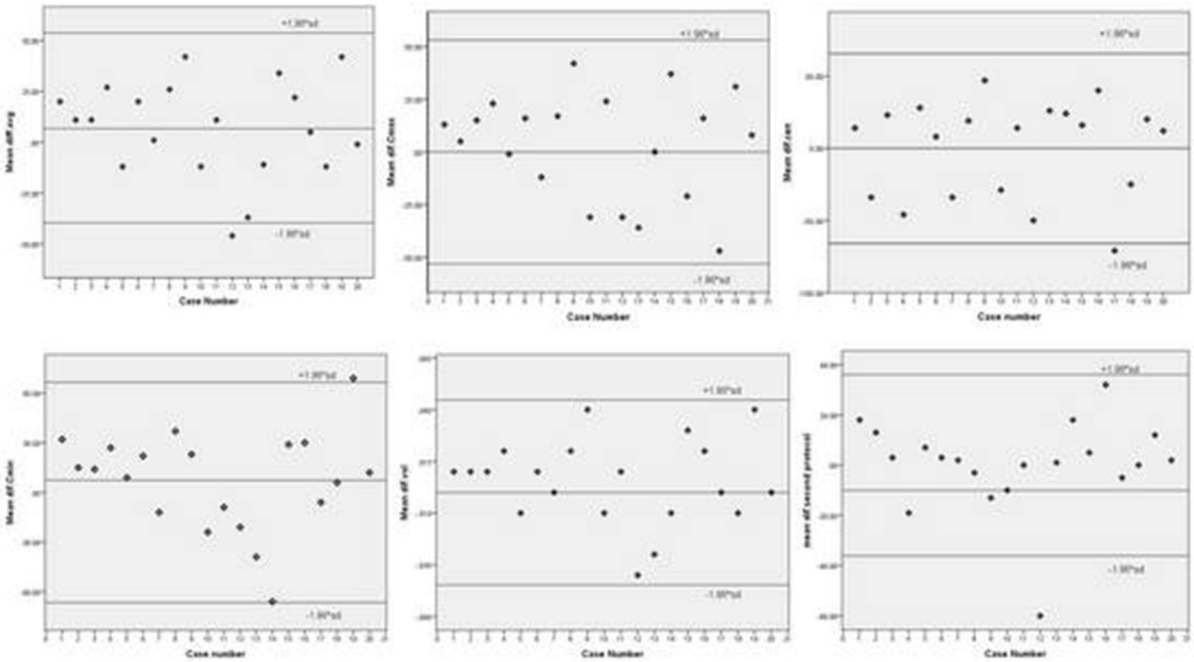

Fig. 4 Bland–Altman plots of mean differences between the two observers' measurements. 95% limits of agreement = mean difference ± 1.96 * SD

Table 3 Intraobserver measurements

	$N = 20$	Intraclass correlation	95% confidence interval	
			Lower bound	Upper bound
Avg	Average measures ND	971	927	989
	Average measures AM	974	934	990
Cen	Average measures ND	947	867	979
	Average measures AM	931	825	973
C_{min}	Average measures ND	925	811	970
	Average measures AM	913	781	966
C_{max}	Average measures ND	969	922	988
	Average measures AM	965	911	986
Vol	Average measures ND	972	928	989
	Average measures AM	971	927	989
Second protocol	Average measures ND	951	877	981
	Average measures AM	994	985	998

Our study found a good interobserver and intraobserver reproducibility in the central ring (1-mm diameter) of Early Treatment Diabetic Retinopathy Study area. Mean SFCT is comparable to the results reported previously. Magnolis et al. [47] included 30 healthy volunteers with a mean age of 50.4 years and found SFCT to be 287 ± 76 µm. Taking the age difference between the two study populations and a mean SFCT decrease of 1.56 µm per year of age into account, Magnolis measurements are in line with our results. In a similar manner, Shao et al. [24] report a mean SFCT of 254.6 ± 107.3 µm and Ding et al. [48]

a mean of 262 ± 88 μm, which are comparable to our results. Other causes for SFCT measurement differences between various studies could be refractive error variations of the study populations and ethnic globe anatomy variations.

We report two techniques of manual choroidal segmentation using the Spectralis OCT built-in automated retinal segmentation EDI software. EDI and eye-tracking functions were utilized in order to acquire good quality and reproducibility of 19 choroidal scans in the raster protocol. Image stabilization with colocalization to a simultaneous infrared scanning laser ophthalmoscope OCT imaging is presumably one of the reasons for the high repeatability that we found. We used segmentation software primarily designed to determine retinal borders to demarcate the choroid and obtained the choroidal thickness measurements by using the same automated software. To our knowledge, there are no previous studies reporting choroidal thickness measurement with the Spectralis OCT instrument, using two different techniques of manual segmentation in EDI mode, in randomly selected patients from a population-based setting regardless of the presence of choroidal pathology.

As it has previously been reported (20), we observed that an average of 25 frames was adequate to give a choroidal image with well-demarcated borders. In most cases EDI-OCT can be used to obtain high-quality choroidal images when measuring choroidal thickness and volume, including 3D imaging. Choroidal thickness measurement by manual segmentation using EDI Spectralis OCT built-in automated retinal segmentation software is highly reproducible and has a very small range of variability when using the above-described methods. Hence, the methodology described may be used to evaluate choroidal thickness in participants in a population-based setting.

Both choroidal segmentation measurement protocols have their advantages and disadvantages. The former is more time-consuming and has a greater learning curve, but provides more information regarding choroidal thickness. The latter is easy and fast to use, but provides a rough estimation of the choroid at a single point. From our experience, both protocols beyond their use in research may have their place in clinical practice, depending on the demand of the patients' needs. However, further research is needed to translate choroidal thickness findings in clinical practice protocols.

Recently, automated choroidal segmentation has been introduced. The majority of these studies include children (34) or young healthy individuals [30, 35, 37]. Some have been conducted in a small number of subjects [49]. In addition, the selected scan for analysis passes through the center of the fovea or close to it [30, 31, 33, 34], giving limited information regarding choroidal pathology in some studies, while others fail to demonstrate observer repeatability [29]. Moreover, the image quality in order to perform the automated choroidal segmentation needs to be higher than in manual [36]. This may consist of an important limitation in the use of automated choroidal segmentation in research involving elderly patients, as well as in clinical practice, where the majority of our patients are elderly with hazy media.

Our study, similar to others, yielded reliability and high reproducibility with the manual nature of segmentation [20, 43]. Our protocols of EDI choroidal thickness measurements may be used in research on elderly population since they provided highly reproducible measurements despite the advanced age of the study population.

Acknowledgements We would like to thank the ophthalmic technicians of the LaRCAO, 1st Department of Ophthalmology, Aristotle University of Thessaloniki, AHEPA Hospital, Irini Lachoura, Evgenia Zamba, Evmorfia Amiridou, Grigoria Tzoanou and Anastasia Rapti for their work and professionalism that greatly assisted the research. We are also grateful to Fei Yu from the Department of Biostatistics, UCLA, who provided advice that greatly assisted the research.

Compliance with ethical standards

Conflict of interest All authors declare that they have no conflict of interest.

Ethical approval All procedures performed were in accordance with the ethical standards of the institutional research committee and with the 1964 Declaration of Helsinki comparable ethical standards.

Informed consent Informed consent was obtained from all individual participants included in the study.

References

1. Hayreh SS (1975) Segmental nature of the choroidal vasculature. Br J Ophthalmol 1975(59):631

2. Nickla DL, Wallman J (2010) The multifunctional choroid. Prog Retin Eye Res 29(2):144–168. https://doi.org/10.1016/j.preteyeres.2009.12.002
3. Ross A, Ross AH, Mohamed Q (2011) Review and update of central serous chorioretinopathy. Curr Opin Ophthalmol 2011(22):166–173
4. Imamura Y, Fujiwara T, Margolis R, Spaide RF (2009) Enhanced depth imaging optical coherence tomography of the choroid in central serous chorioretinopathy. Retina 2009(29):1469–1473
5. Chung SE, Kang SW, Lee JH, Kim YT (2011) Choroidal thickness in polypoidal choroidal vasculopathy and exudative age-related macular degeneration. Ophthalmology 2011(118):840–845
6. Ting DS, Ng WY, Ng SR, Tan SP, Yeo IY, Mathur R, Chan CM et al (2016) Choroidal thickness changes in age-related macular degeneration and polypoidal choroidal vasculopathy: a 12-month prospective study. Am J Ophthalmol 164:128. https://doi.org/10.1016/j.ajo.2015.12.024
7. Yannuzzi LA, Sorenson J, Spaide RF, Lipson B (1990) Idiopathic polypoidal choroidal vasculopathy (IPCV). Retina 1990(10):1–8
8. Koizumi H, Yamagishi T, Yamazaki T, Kawasaki R, Kinoshita S (2011) Subfoveal choroidal thickness in typical age-related macular degeneration and polypoidal choroidal vasculopathy. Graefes Arch Clin Exp Ophthalmol 2011(249):1123–1128
9. Zheng F, Gregory G, Schaal KB, Legarreta AD, Miller AR, Roisman L et al (2016) Choroidal thickness and choroidal vessel density in nonexudative age-related macular degeneration using swept-source optical coherence tomography imaging. Invest Ophthalmol Vis Sci 57(14):6256–6264. https://doi.org/10.1167/iovs.16-20161
10. Koizumi H, Kano M, Yamamoto A, Saito M, Maruko I, Sekiryu T et al (2016) Subfoveal choroidal thickness during aflibercept therapy for neovascular age-related macular degeneration: 12-month results. Ophthalmology 123(3):617–624. https://doi.org/10.1016/j.ophtha.2015.10.039
11. Fong AH, Li KK, Wong D (2011) Choroidal evaluation using enhanced depth imaging spectral-domain optical coherence tomography in Vogt-Koyanagi-Harada disease. Retina 2011(31):502–509
12. Read RW, Rao NA, Cunningham ET (2000) Vogt-Koyanagi-Harada disease. Curr Opin Ophthalmol 2000(11):437–442
13. Maruko I, Iida T, Sugano Y, Go S, Sekiryu T (2011) Subfoveal choroidal thickness after treatment of Vogt-Koyanagi-Harada disease. Retina 2011(31):510–517
14. Fujiwara T, Imamura Y, Margolis R, Slakter JS, Spaide RF (2009) Enhanced depth imaging optical coherence tomography of the choroid in highly myopic eyes. Am J Ophthalmol 2009(148):445–450
15. Aoyagi R, Hayashi T, Masai A, Mitooka K, Gekka T, Kozaki K et al (2012) Subfoveal choroidal thickness in multiple evanescent white dot syndrome. Clin Exp Optom 2012(95):212–217
16. Comyn O, Heng LZ, Ikeji F, Bibi K, Hykin PG, Bainbridge JW et al (2012) Repeatability of spectralis OCT measurements of macular thickness and volume in diabetic macular edema. Invest Ophthalmol Vis Sci 53(12):7754–7759. https://doi.org/10.1167/iovs.12-10895
17. Bressler SB, Edwards AR, Chalam KV, Bressler NM, Glassman AR, Jaffe GJ et al (2014) Reproducibility of spectral-domain optical coherence tomography retinal thickness measurements and conversion to equivalent time-domain metrics in diabetic macular edema. JAMA Ophthalmol 132(9):1113–1122. https://doi.org/10.1001/jamaophthalmol.2014.1698
18. Ikuno Y, Maruko I, Yasuno Y, Miura M, Sekiryu T, Nishida K et al (2011) Reproducibility of retinal and choroidal thickness measurements in enhanced depth imaging and high-penetration optical coherence tomography. Invest Ophthalmol Vis Sci 2011(52):5536–5540
19. Rahman W, Chen FK, Yeoh J, Patel P, Tufail A, Da Cruz L (2011) Repeatability of manual subfoveal choroidal thickness measurements in healthy subjects using the technique of enhanced depth imaging optical coherence tomography. Invest Ophthalmol Vis Sci 2011(52):2267–2271
20. Chhablani J, Barteseli G, Wang H, El-Emam S, Kozak I, Doede AL et al (2012) Repeatability and reproducibility of manual choroidal volume measurements using enhanced depth imaging optical coherence tomography. Invest Ophthalmol Vis Sci 53(4):2274–2280. https://doi.org/10.1167/iovs.12-9435
21. Yamashita T, Yamashita T, La ShirasawDa Cruz M, Arimura N, Terasaki H, Sakamoto T (2012) Repeatability and reproducibility of subfoveal choroidal thickness in normal eyes of Japanese using different SD-OCT devices. Invest Ophthalmol Vis Sci 53(3):1102–1107. https://doi.org/10.1167/iovs.11-8836
22. Shao L, Xu L, Zhang JS, You QS, Chen CX et al (2015) Subfoveal choroidal thickness and cataract: the Beijing Eye Study 2011. Invest Ophthalmol Vis Sci 56(2):810–815. https://doi.org/10.1167/iovs.14-15736
23. Karaca EE, Özdek Ş, Yalçin NG, Ekici F (2014) Reproducibility of choroidal thickness measurements in healthy Turkish subjects. Eur J Ophthalmol 24(2):202–208. https://doi.org/10.5301/ejo.5000351
24. Shao L, Xu L, Chen CX, Yang LH, Du KF, Wang S et al (2013) Reproducibility of subfoveal choroidal thickness measurements with enhanced depth imaging by spectral-domain optical coherence tomography. Invest Ophthalmol Vis Sci 54(1):230–233. https://doi.org/10.1167/iovs.12-10351
25. Patel PJ, Chen FK, Ikeji F, Xing W, Bunce C, Da Cruz L et al (2008) Repeatability of stratus optical coherence tomography measures in neovascular age-related macular degeneration. Invest Ophthalmol Vis Sci 49(3):1084–1088. https://doi.org/10.1167/iovs.07-1203
26. Patel PJ, Chen FK, Ikeji F, Tufail A (2011) Intersession repeatability of optical coherence tomography measures of retinal thickness in early age-related macular degeneration. Acta Ophthalmol 89(3):229–234. https://doi.org/10.1111/j.1755-3768.2009.01659.x
27. Kim JS, Knickelbein JE, Jaworski L, Kaushal P, Vitale S, Nussenblatt RB et al (2016) Enhanced depth imaging optical coherence tomography in uveitis: an intravisit and interobserver reproducibility study. Am J Ophthalmol 164:49–56. https://doi.org/10.1016/jajo.2016.01.004

28. Sim DA, Keane PA, Mehta H, Fung S, Zarranz-Ventura J, Fruttiger M et al (2013) Repeatability and reproducibility of choroidal vessel layer measurements in diabetic retinopathy using enhanced depth optical coherence tomography. Invest Ophthalmol Vis Sci 54(4):2893–2901. https://doi.org/10.1167/iovs.12-11.085
29. Hu Z, Wu X, Ouyang Y, Ouyang Y, Sadda SR (2013) Semiautomated segmentation of the choroid in spectral-domain optical coherence tomography volume scans. Investig Ophthalmol Vis Sci 54(3):1722–1729
30. Tian J, Marziliano P, Baskaran M, Tun TA, Aung T (2013) Automatic segmentation of the choroid in enhanced depth imaging optical coherence tomography images. Biomed Opt Express 4(3):397–411
31. Lu H, Boonarpha N, Kwong MT, Zheng Y (2013) Automated segmentation of the choroid in retinal optical coherence tomography images. In: IEEE 35th Annual International Conference of the Engineering in Medicine and Biology Society (EMBC). p 5869–72
32. Kajíc V, Esmaeelpour M, Považay B, Marshall D, Rosin PL, Drexler W (2012) Automated choroidal segmentation of 1060 nm OCT in healthy and pathologic eyes using a statistical model. Biomed Opt Express 3(1):86–103
33. Danesh H, Kafieh R, Rabbani H, Hajizadeh F. (2014) Segmentation of choroidal boundary in enhanced depth imaging OCTs using a multiresolution texture based modeling in graph cuts. Comput Math Methods Med
34. Alonso-Caneiro D, Read SA, Collins MJ (2013) Automatic segmentation of choroidal thickness in optical coherence tomography. Biomed Opt Express 4(12):2795–2812
35. Twa MD, Shulle KL, Chiu SJ, Farsiu S, Berntsen DA (2016) Validation of macular choroidal thickness measuremesmaeelpour ents from automated SD-OCT image segmentation. Optom Vis Sci 93(11):1387–1398
36. Gupta P, Jing T, Marziliano P, Cheung CY, Baskaran M, Lamoureux EL et al (2015) Distribution and determinants of choroidal thickness and volume using automated segmentation software in a population-based study. Am J Ophthalmol 159(2):293. https://doi.org/10.1016/j.ajo.2014.10.034
37. Zhang L, Lee K, Niemeijer M, Mullins RF, Sonka M, Abràmoff MD (2012) Automated segmentation of the choroid from clinical SD-OCT. Invest Ophthalmol Vis Sci 53(12):7510–7519. https://doi.org/10.1167/iovs.12-10311
38. Topouzis F, Coleman A, Harris A, Anastasopoulos E, Yu F, Koskosas A et al (2006) Prevalence of age-related macular degeneration in Greece: the Thessaloniki Eye Study. Am J Ophthalmol 142(6):1076–1079
39. Springelkamp H, Lee K, Wolfs RC, Buitendijk GH, Ramdas WD, Hofman A et al (2014) Population-based evaluation of retinal nerve fiber layer, retinal ganglion cell layer, and inner plexiform layer as a diagnostic tool for glaucoma. Invest Ophthalmol Vis Sci 55(12):8428–8438
40. Group E (1991) Early Treatment Diabetic Retinopathy Study Research Group.ETDRS report number 10. Grading diabetic retinopathy from stereoscopic color fundus photographs—an extension of the modified Airlie House classification. Ophthalmology 1991(98):786–806
41. Bland JM, Altman DG (1986) Statistical methods for assessing agreement between two methods of clinical measurement. Lancet 1986(1):307–310
42. Guyer DR, Puliafito CA, Mones JM, Friedman E, Chang W, Verdooner SR (1992) Digital indocyanine-green angiography in chorioretinal disorders. Ophthalmology 1992(99):287–291
43. Adhi M, Liu JJ, Qavi AH, Grulkowski I, Lu CD, Mohler KJ et al (2014) Choroidal analysis in healthy eyes using swept-source optical coherence tomography compared to spectral domain optical coherence tomography. Am J Ophthalmol 157(6):1272. https://doi.org/10.1016/j.ajo.2014.02.034
44. Spaide RF, Koizumi H, Pozzoni MC (2008) Enhanced depth imaging spectral-domain optical coherence tomography. Am J Ophthalmol 146(4):496–500. https://doi.org/10.1016/j.ajo2008.05.032
45. Shin JW, Shin YU, Lee BR (2012) Choroidal thickness and volume mapping by a six radial scan protocol on spectral-domain optical coherence tomography. Ophthalmology 119(5):1017–1023. https://doi.org/10.1016/j.ophtha.2011.10.029
46. Chhablani J, Barteseli G, Bartsch DU, Kozak I, Wang H, El-Emam S et al (2013) Influence of scanning density on macular choroidal volume measurement using spectral-domain optical coherence tomography. Graefes Arch Clin Exp Ophthalmol 251(5):1303–1309. https://doi.org/10.1007/s00417-012-2188-0
47. Margolis R, Spade RF (2009) A pilot study of enhanced depth imaging optical coherence tomography of the choroid in normal eyes. Am J Ophthalmol 2009(147):811–815
48. Ding X, Li J, Zeng J, Ma W, Liu R et al (2011) Choroidal thickness in healthy Chinese subjects. Invest Ophthalmol Vis Sci 2011(52):9555
49. Vupparaboina KK, Nizampatnam S, Chhablani J, Richhariya A, Jana S (2015) Automated estimation of choroidal thickness distribution and volume based on OCT images of posterior visual section. Comput Med Imaging Graph 3:315–327. https://doi.org/10.1016/j.compmedimag.2015.09.008